Model experiments on geosynthetic reinforced piled embankments, 3D test series

S.J.M. van Eekelen[1,2] and A. Bezuijen[1,3]
Deltares[1], Delft University of Technology[2] and Ghent University[3]

Abstract: In the Netherlands, several field measurements were carried out in piled embankments with a geosynthetic basal reinforcement (GR). This paper presents a series of nineteen 3D model experiments on piled embankments. Purpose of the tests was to find an explanation why the calculated GR strains exceed the GR strains measured in the field.
This paper focuses on the starting points of the test series, the test set-up and the scaling rules and gives a summary of the results. Van Eekelen et al., (2011b and 2011c) describe the results of the tests extensively. Five starting points were leading to the development of the test set-up. (1) Possibility to evaluate the two calculation steps separately, (2) Possibility to evaluate the influence of consolidation of the subsoil, (3) Inclusion of GR, (4), Modelling the fill realistically, (5) a realistic stress level and scale.
For the test conditions (static load, laboratory scale), it was found that consolidation of the subsoil results in an increase of arching. This is not in agreement with the current calculation models. Loading on the GR is concentrated on the strips lying above and between adjacent piles (the "GR strips") which is in agreement with the current calculation models. The measured load on a GR strip has the distribution of an inverse triangle, although the load may be even more concentrated around the pile caps than this indicates. This is not in agreement with the current calculation models. Implementing this in the CUR/EBGEO calculation model results in 19-26% less GR strain.

Keywords: Geosynthetic reinforcement, piled embankments, experiments, arching, membranes

1 INTRODUCTION

In 2010, new or updated design guidelines for piled embankments were published in the Netherlands, Germany, and the United Kingdom (respectively CUR226 [2010], described in English in Van Eekelen et al., [2010b]; EBGEO [2010]; and BS8006-1 [2010]). In the Netherlands, this was the first result of an ongoing research and development programme, which includes laboratory and field tests aimed at improving understanding of the arching mechanism, investigating the factors of influence, and further optimisation of the Dutch CUR Design Guideline.

For this Dutch research program, the results of several full scale monitoring projects were evaluated, for example the N210 (Haring et al., 2008) and a railway at Houten in the Netherlands (Van Duijnen et al., 2010). In these measurements, all measured strains appeared to be much smaller than the strains predicted by any of the above-mentioned guidelines.

This paper presents a series of laboratory tests on piled embankments. The purpose of these tests was to find an explanation for the relatively small strains in comparison with predictions with the available design models and if possible, modify the calculation models to improve the agreement between measurements and calculations. Van Eekelen et al., 2012[a] and 2012[b] also published about these test series. They focussed on the results. This paper focuses on the test set-up and scaling.

The next section gives a brief summary of most design models. After that, starting points for the test series are discussed, leading to the test set-up presented in section 4. The paper continues with presenting the main results leading to suggestions for modifications of the calculation models of CUR and EBGEO.

2 DESIGN OF THE GEOSYNTHETIC REINFORCEMENT IN A PILED EMBANKMENT

A basal reinforced piled embankment consists of a field of piles with (or sometimes without) pile caps and an embankment (fill) that is reinforced at the base with a geosynthetic. This paper considers the design of this geosynthetic reinforcement (GR). All considered design methods (CUR 226, 2010, EBGEO, 2010 and BS8006, 2010) consider the influence of the vertical load (traffic load, soil weight) and the horizontal load (breaking forces, spreading forces, centrifugal forces etcetera) separately. This paper only considers the consequences of the vertical load.

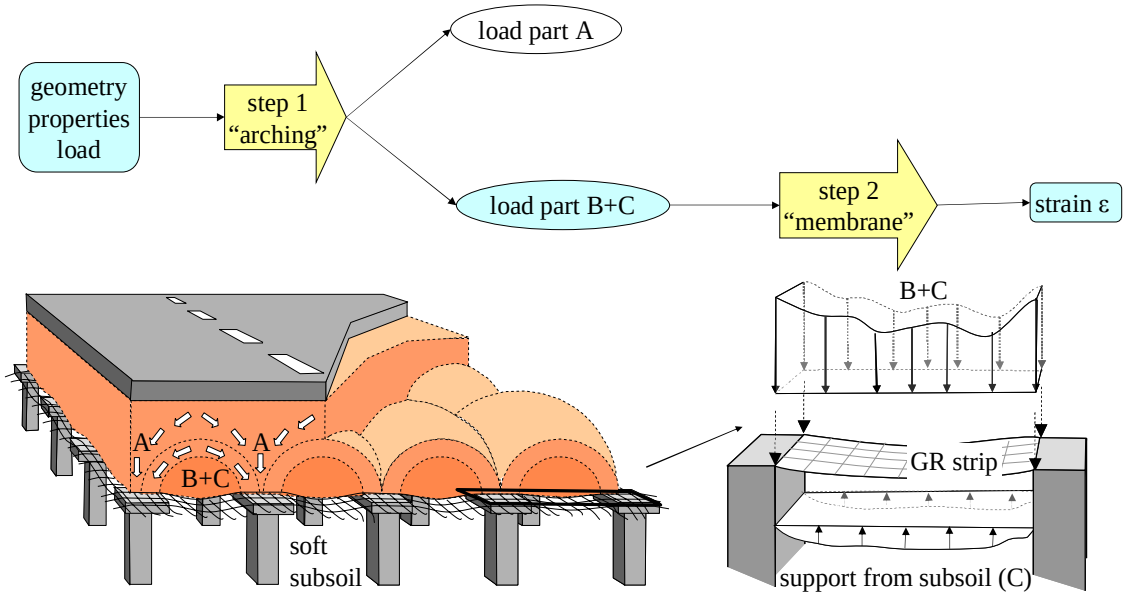

Figure 1. In most design methods, the calculation of the GR strain due to vertical load is carried out in two steps.

The calculation of the GR strains from the vertical load is carried out in two steps, as shown in Figure 1. In the first step, the vertical load is divided into two parts. The first part is transferred to the piles directly, and called 'A' (kN/pile). The second part is the 'rest'. In Figure 1 this 'rest' is called 'B+C'. Part A is relatively large due to arching. Therefore, this step 1 is called the 'arching step'. Both EBGEO and CUR226 adopted Zaeske's model (Zaeske, 2001) for this calculation step. BS8006 adopted Marston's (1913) model, and modified this model to get a 3D model (as described in Van Eekelen, 2011a and Lawson, 2012).

In step 2, it is assumed that the GR strip between two piles is normative for the GR design. In other words, it is assumed that the strains occur mainly in this strip. Assuming some load distribution on this GR strip, and if possible, some support from the subsoil, the GR strain ε can be calculated. CUR and EBGEO calculate with a triangular distribution of the load on the GR strip, while BS8006 chose for an equally distributed load, and does not allow calculating with subsoil support. However, Lawson (2012) suggests considering the equally distributed vertical load a net value.

Step 2 implicitly results in a further division of the vertical load, as shown in Figure 2; load A goes directly to the piles (arching), load B is transferred through the GR to the piles and load C is carried by the subsoil. It should be noted that load A, B and C are expressed in kN/pile and that A, B and C are vertical loads.

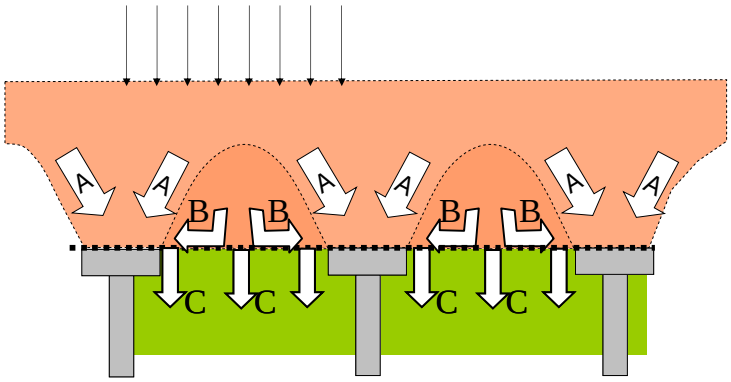

Figure 2. Load distribution in a piled embankment.

3 STARTING POINTS FOR THE TEST SERIES

Five starting points were leading in the development of the test set-up. They will be discussed separately in the following sections.

3.1 Possibility to evaluate calculation steps 1 and 2 separately

Starting point was that it had to be possible to evaluate calculation steps 1 and 2 separately (see section 2). Therefore, it is necessary to measure the load distribution and the GR strains.

3.1.1 Measuring the load distribution

The forces on or below the piles were often measured, see Low et al., 1994; Zaeske, 2001; Heitz, 2006; Farag, 2008; Chen et al., 2008 and Ellis and Aslam, 2009a and 2009b and Blanc et al. (2012). These researchers have measured A+B. Some researchers measured the pressures within the fill (Zaeske, 2001; and Heitz, 2006). The distribution of the load over the subsoil (C), the reinforcement (B), and the piles (A) was never measured separately. This is necessary to be able to validate step 1 and 2 separately. In the test series presented in this paper, a new feature was that it was possible to measure A, B and C separately, as presented in section 4.1.

3.1.2 Measuring deformations and strains

Many researchers observed arching through a glass wall (such as Hewlet and Randolph, 1988; Low et al., 1994; Chen et al, 2008, Jenck et al., 2009; and Ellis and Aslam, 2009a and 2009b), and some measured settlement at some locations, like Zaeske (2001), Heitz (2006) and Blanc et al. (2012). It is difficult to attach strain gauges to geosynthetics and to interpret them. In addition, they frequently influence the stiffness of the geosynthetic by locally "reinforcing" the GR and interpretation of data can be difficult as the GR stiffness may vary in the main stress direction. Furthermore, strain gauges often fail before the strains become interesting. Glue does not adhere to most geosynthetics. Therefore, the GR strains were usually not measured, with the exception of Zaeske (2001) and Heitz (2006). In this paper, a new method is presented to measure GR strains, as presented in section 4.2.

3.2 Possibility to evaluate the influence of consolidation of the subsoil

It is necessary to model consolidation (or settlements) of the subsoil in an experiment on piled embankments to let the arching develop. Several researchers simply took away subsoil support during the test, either via a 'trap door' (Horgan and Sarsby, 2002) or by removal (Le Hello, 2007). Most others forced compression of the subsoil by applying peat (Zaeske, 2001; Heitz, 2006; and later Farag, 2008), rubber foam (the 2D tests of Jenck et al., 2009, Low et al, 1994 and Van Eekelen et al., 2003), or rubber foam chips (Hewlet and Randolph, 1988). Ellis and Aslam (2009a and 2009b) varied the stiffness of the

subsoil by applying two grades of EPS in their centrifuge tests. Blanc et al. (2012) modelled in their centrifuge tests the settling subsoil with a steel plate that was lowered displacement-controlled.

Chen et al. (2008) modelled the consolidation of the subsoil in their 2D tests by permitting water to flow out gradually from water bags. No researchers chose to control or to measure the subsoil support.

In the tests presented in this paper, the subsoil was modelled with a watertight wrapped soaked foam cushion, as described in section 4.1. This way, it was possible to control and measure the subsoil support. The deflection of the subsoil and GR was induced by the pressure from the fill.

3.3 Inclusion of geosynthetic reinforcement (GR)

A limited number of researchers included geosynthetic reinforcement (GR) in their experiments, namely Zaeske, 2001, Heitz, 2006, Le Hello, 2007, Chen et al., 2008 and Blanc et al., 2012. The reason for not including is probably the complexity to attach the GR, and on the other hand the conviction that the presence of GR does not influence the arching mechanism. The authors of this paper believe that the arching is improved by the application of GR. In the experiments presented in this paper, GR was therefore included. It was attached to a steel frame that could move vertically during the tests. Differential settlements along the frame were not possible.

3.4 Modelling the fill as realistic as possible

All three above mentioned design guidelines require the application of a frictional fill. In the Netherlands, the bottom layer of the fill is usually constructed with crushed, recycled construction material (concrete, bricks, from now on called ‘granular material’). Usually the size of the grains lies between 0 and 40 mm. It is a starting point to keep as close as possible to this rough material type and to evaluate the difference with the application of sand.

The majority of researchers used a fill of dry or moist sand, except for Horgan and Sarsby (2002) who applied additionally 10 mm gravel in their ‘trap door’ tests. Jenck et al. (2009) used a mix of steel rods measuring 3, 4 and 5 mm in diameter and 60 mm in length. The model is therefore two-dimensional.

In the tests presented in this paper, a granular fill was used to model the three-dimensional interaction between a geogrid and granular material optimal. Only in two of the nineteen tests, sand was applied for comparison reasons.

3.5 Realistic stress level and scale

For the determination of the scale of the test and the stress level in the test, two starting points were important.

1. The scale of the test had to be suitable for carrying out several tests economically. Therefore, it was necessary to be able to carry out one test each week.
2. The stresses in the test had to be realistic to avoid complications due to stress dependent behaviour. Therefore, the stresses have to be the same in model and prototype.

3.5.1 Suitable scale

It was chosen to adopt the scale of the tests of Zaeske (2001) and Heitz (2006) that had a suitable size for carrying out a test each week.

The centre-to-centre pile distances applied in Dutch practice are currently between 0.9 and 2.50 m. The centre-to-centre distance of the piles in the test series was 0.55 m. Therefore, the dimensions of the test set-up are smaller by a factor of approximately 1.6 to 4.5 compared to field applications.

Table 1 gives the scaling rules between the tests and the prototype, adopting a realistic vertical stress as a starting-point (section 3.5.2), thus stress (kN/m^2) scale = 1:1. It should be noted that the strength and tensile modulus are scaled down by a factor of 1:x, while the mesh-size of each grid was kept constant. This may have an influence on the load-transfer on top of the piles.

Table 3 shows the dimensions of a test set-up with a scale of 1:3. It should be noted that it is not necessary to use these scaling rules for calculations and when analysing the test series. If the calculation model is correct, this should work for both prototype and model dimensions.

Table 1. Scaling.

			test/prototype scale 1:x
length		m	1:x
area	length *length	m^2	$1:x^2$
stress	force / area	kN/m^2	1:1
force[a]	stress x area	kN	$1:x^2$
tensile strength GR[b]	force / length	kN/m	1:x
tensile stiffness GR[b]	force / length	kN/m	1:x
(deflection GR)/(distance between the piles)		m/m	1:1

[a] "Force" refers to the force on the pile head

[b] Tensile strain and strength refer to the geosynthetic

3.5.2 Realistic stresses

Starting point was to work with realistic average vertical stresses (scale 1:1) in the normative part of the fill, which is the area directly above the GR. This starting point is chosen in order to avoid complications due to stress dependent behaviour. First, it is determined what stresses are realistic in several applications.

Roads and highways

The Dutch Guideline gives rules how to translate the load of a now and then passing truck into a uniformly distributed (input-)load, as described in Van Eekelen et al., 2010a.

The load of the wheels is spread according Boussinesq over the total height of the embankment. The influence of the wheels of all three axles of a standard truck is summed. The design value for the surcharge load ($\sigma_{max;ave}$) is the average stress on the maximal loaded pile grid ($s_x \cdot s_y$), with $s_{x,y}$ (m) the centre-to-centre (CTC) distance between piles. Table 3 presents a summary of a larger table from CUR226 (2010) with these design loads. These values are determined for a 'standard truck' of 600 kN.

Table 3 also gives the resulting average load on GR level, assuming a unit soil weight γ = 18 kN/m^3.

Table 2. Example scale 1:3

	test	prototype
model box	1.1 x 1.1 m^2	3.3 x 3.3 m^2
diameter piles	0.1 m	0.3 m
centre-to-centre (CTC) distance piles	0.55 m	1.65 m
embankment height	0.42 m	1.26 m
tensile strength GR (in representative test K2)	135 kN/m	405 kN/m
tensile stiffness GR ($J_{2\%}$ in test K2)	2269 kN/m	6807 kN/m

Table 3. Surcharge load on roads: calculation examples of surcharge load for a 600 *kN* truck (source: CUR 226, 2010), and the resulting average vertical stress at GR level, assuming a unit soil weight γ = 18 kN/m^3.

	surcharge load $\sigma_{max;ave}$ (kPa)			average vertical stress on GR level $\sigma_{GR,ave}$ (kPa)		
CTC distance piles height embankment (m)	1.5 x 1.5 m²	2.0 x 2.0 m²	2.5 x 2.5 m²	1.5 x 1.5 m²	2.0 x 2.0 m²	2.5 x 2.5 m²
1.0	61.3	51.3	44.8	79.3	69.3	62.8
2.0	33.7	30.0	27.8	69.7	66	63.8
3.0	21.1	19.8	19.0	75.1	73.8	73
4.0	15.1	14.6	14.2	87.1	86.6	86.2
5.0	11.9	11.6	11.5	101.9	101.6	101.5

Railways

In Dutch railway projects, the principle, ProRail, requires a design load of 43 kPa. Adding the weight of an embankment results in average vertical stresses on GR level as given in Table 4.

Table 4. Surcharge load on railways: calculation examples of resulting average vertical stress at GR level, given the required surcharge load of 43 kPa, and assuming a unit soil weight $\gamma = 18$ kN/m^3.

height embankment H (m)	1.0	2.0	3.0	4.0	5.0
average vertical stress on GR level $\sigma_{GR,ave}$ (kPa)	61	79	97	115	133

The actual measured passage of a heavy crane was measured in a railway in the Netherlands. According to the CUR 226-rules, this crane plus the embankment weight results in a stress on GR level of 90 kPa. This finding is compared with the measured loads on the piles during the crane passage, with satisfying results, as reported in Van Duijnen et al., 2010.

Other applications

Occasionally, piled embankments are constructed for purposes different from normal roads or railways. Examples are platforms for heavy cranes or storage areas for containers or other materials. In the experience of the authors, the exceptional required design values for surcharge loads exceed in these cases up to 260 kPa for an extremely heavily loaded crane footing and 113 kPa for a container terminal. The weight of the embankments should be added as done in Table 3.

Conclusions

It is found that the average vertical stress on GR level varies between 61 and 97 kPa for roads and railways with a height of 3 meters or less. Relatively thin embankments (≤ 3 meter) are considered normative and therefore, the maximum surcharge load in the tests is chosen to be 100 kPa. This applied surcharge load represents both the traffic load and the weight of the top layer of the embankment in the prototype.

It is chosen to increase the surcharge load during each test. Between the load steps, the subsoil support is decreased in steps. This way, several combinations of surcharge load and subsoil support can be evaluated.

The maximum top load was not the same in all tests. During the first tests only 50 kPa was applied, which was necessary to test the test set-up. Table 5 compares the maximum top load of 100 kPa with the top load in the prototype.

Table 5. Scaling surcharge load and determination prototype static traffic load.

	test	prototype
top load	100 kPa	100 kPa
weight fill $\gamma \cdot H$	$20 \cdot 0.42 = 8.4$ kN/m^2	$20 \cdot 1.26 = 25.2$ kN/m^2
traffic load		$100 - 25.2 + 8.4 = 83.2$ kN/m^2

4TEST SET-UP AND MEASUREMENTS

4.1 Test set-up

Nineteen tests were conducted using the test set-up shown in Figure 3. A steel plate supports a cushion that models the soft soil (hereafter called ‘subsoil’) around the piles. This cushion is a watertight, soaked foam rubber cushion (hereafter called ‘foam cushion’). A tap allows drainage of the cushion during the test, which models the consolidation process of the soft soil.

The four ’piles’ extend through the steel plate and rest on the bottom of the box. A sand layer measuring between 0.015 and 0.02 m is placed on top of the foam cushion and the piles. One or two stiff steel frames are placed on top of this, to which the geosynthetic reinforcement (GR) is attached. If two

steel frames with GR are used, 0.05 or 0.10 m of granular material is placed in between. The embankment is a layer of sand or granular fill, in most tests, the fill had a height of 0.42 m . The top load is applied by means of a water cushion. This provides an equally distributed top load, even when the ground level deforms. The applied top load represents both the traffic load and the weight of the top layer of the embankment. A rubber sheet combined with Vaseline or Shell Retinax A minimises the friction between the fill, the box walls, the foam cushion and the piles.

The tests reported in this paper are similar to those of the Kempfert group, as reported by Zaeske (2001) and Heitz (2006) for example. In the test series reported here, however, the fill was granular material instead of sand, the subsoil support was controlled by means of the foam cushion, and the load distribution was measured differently. This allowed the influence of subsoil loading on the load parameters A and B to be tested. Another difference was that load parts A, B and C could be measured separately.

4.2 Measurements

The general measurement set-up is presented in Figure 4, although the number of transducers and their exact location differ for each test. In addition to what is shown in Figure 4, the pressure in both cushions, and the amount of water drained from the foam cushion are also measured.

Load parts A and B were measured using total pressure cells with a diameter equal to the pile diameter of 0.1 m. In all tests, two total pressure cells measured A + B. They were located below the reinforcement, on top of the piles.

For measuring load part B, two types of tests are distinguished: tests with only one reinforcement layer in one frame (hereafter called ‘single-layered tests’), and tests with two reinforcement layers in two frames (hereafter called ‘double-layered tests’). This paper presents the single-layered tests only.

In the single-layered tests (see Figure 3c), load part A was measured by total pressure cells positioned above a pile and on top of the GR. Load part B was found by subtraction i.e. B = (A+B)-A. Where loads were measured at two locations, the average is given in the results.

Load part C was determined by measuring the pressure in the foam cushion.

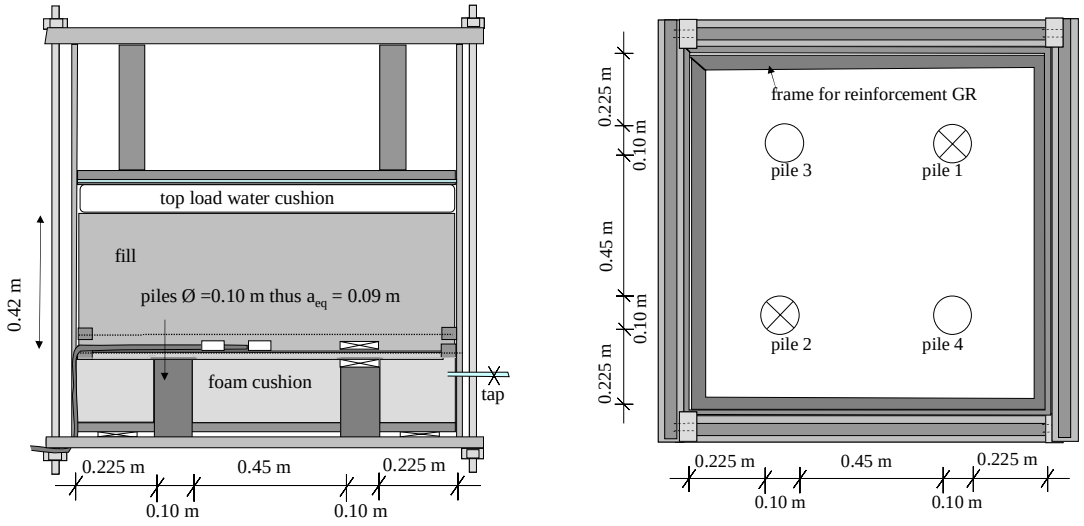

Figure 3. Side view and top view of test set-up

Vertical deflection of the reinforcement was measured using a liquid levelling system.

One type of grid (used in tests N1, N2 and N3) was suitable for the adherence of traditional strain gauges due to its flat and monolithic bars. They gave convincing results up to approximately 4% GR strain. By applying the strain gauges on the bottom as well as on top of the bars, bending normalised total medium strain could be measured.

In the other tests, strains within the geosynthetic were measured using bicycle gear cables, hereafter called ‘strain cables’ (shown in Figure 5). In most tests, six of those strain cables were attached to the reinforcement with cable ties. Displacement transducers registered the difference between displacement

of the inner cable and the outer tube. Results appeared to depend on fixation of the outer gear cable over the whole of the GR and pre-stress in the cable. The results from the strain cables were consistent, but were too high in the first tests. In addition, GR strains measured locally were strongly dependent on the exact location of the strain cable or strain gauge. For both these reasons, the results of the strain cables were only considered qualitatively throughout the tests. Most 'measured GR strains' presented in this paper were calculated using the measured deflection of the GR, assuming a third-order-polynomial-shaped deformed GR as shown in Figure 8.

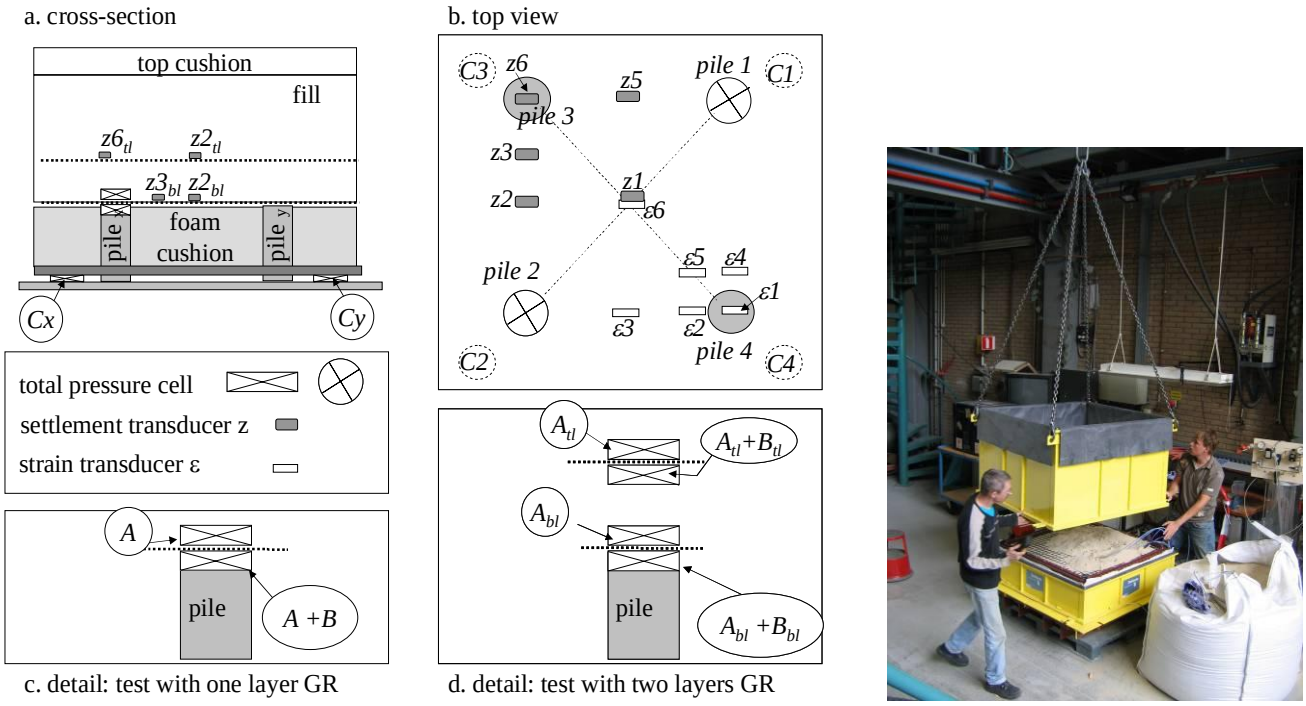

Figure 4. Nomenclature of measurements: 'tl' indicates 'top grid layer', and 'bl' indicates 'bottom grid layer'

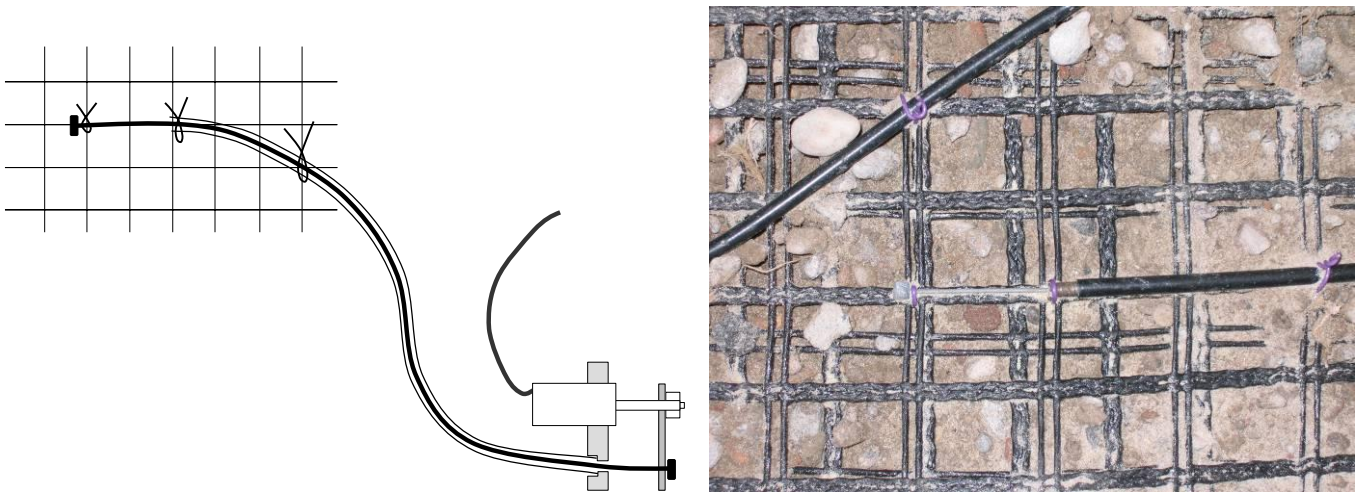

Figure 5. Gear cable to measure strains in the reinforcement

4.3 Test procedure

After the fill was in place, the following steps were carried out in each test: (1) drainage of the foam cushion (modelling subsoil consolidation); (2) the first increase in top load, usually up to 25 kPa; (3) one or more subsequent drainage steps; (4) second top load increase; usually up to 50 kPa (5) one or more drainage steps; (6) third top load increase; (7) one or more drainage steps; continuing until the maximum top load had been reached and the subsequent drainage steps were completed.

In some tests, vacuum pressure was then applied to the foam cushion below the GR to suck it away from the GR, until the resulting load part C had been reduced to zero. The test procedure represents a stepwise increase in load, and subsequent consolidation of the subsoil underneath the piled embankment. After each drainage step or top load increase, the system was allowed to stabilise for several hours or sometimes throughout the night, until the measurements became stable. This was necessary so that the foam cushion had time to consolidate.

5 RESULTS

The results of the first 12 tests are described, analysed and compared with CUR/EBGEO calculations extensively in Van Eekelen et al., 2011b and 2011c. This paper gives the most important conclusions.

5.1 Results step 1

As shown in section 2, calculation step 1 divides the vertical load into two parts: A and B+C. Figure 6 compares the measured and calculated resulting load part A. The figure shows that A follows a smoothly ascending curve when plotted against net load. The figure also shows that consolidation of the subsoil results in increased measured arching (A) in the fill. Consolidation (subsoil deformation) is obviously necessary for the development of arching.

According to EBGEO, consolidation of the subsoil leads to no increase in arching. This results in a calculated value for arching load part A that is lower than shown in the model tests, and in turn gives a calculation for load part B+C (and thus GR strain) that is higher than shown in the model tests. The improvement of step 1 is a subject for further study, and will be published at a later date.

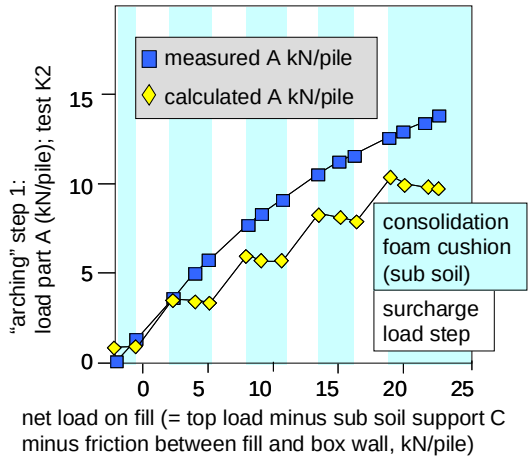

Figure 6. Measured and calculated (CUR/EBGEO) result of step 1 (arching)

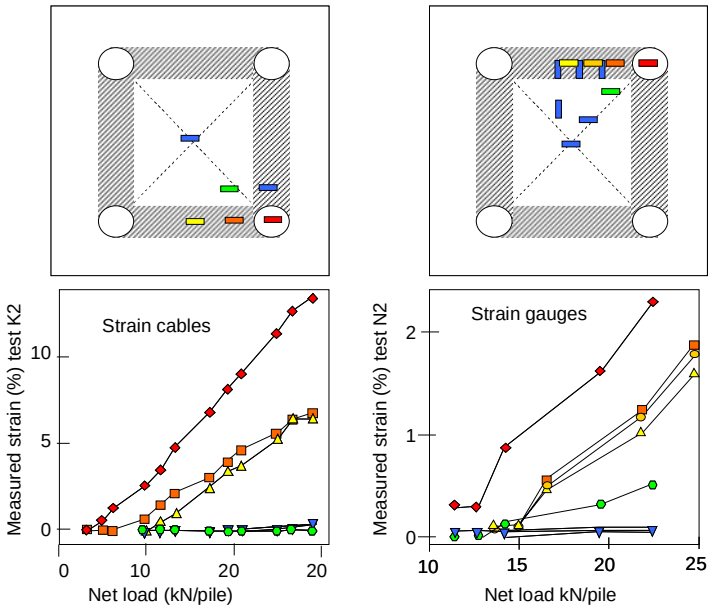

Figure 7. Measured strains occur mainly in the tensile strips that lie on the GR strip between adjacent piles, in accordance with the calculation models (see Figure 1),

5.2 Results step 2

Calculation step 2 (membrane step), consists of two parts. Firstly, the assumption is made that the GR strains occur mainly in the GR strips as shown in Figure 1. Figure 7 confirms this first assumption: all tests show that the GR strains occur mainly in the tensile strips that lie on top of and between adjacent piles. The assumption is also proven by numerical simulations of the test series (Den Boogert, et al., 2012) and several authors report the same results of their numerical calculations (Jones et al., 2010 and Halvordson et al, 2010).

EBGEO calculations do not take GR strains on the pile caps into account, although these can be the largest GR strains under specific conditions, such as for the smooth, small-diameter pile caps in the test set-up. As this will generally not be the case in the field, it was decided not to modify the step 2 calculations because of this conclusion.

The loading and supporting of the GR strip is considered in the second part of step 2, as shown in Figure 1. The load distribution on the strip is directly related to the deformed shape of the GR, as shown in Figure 8

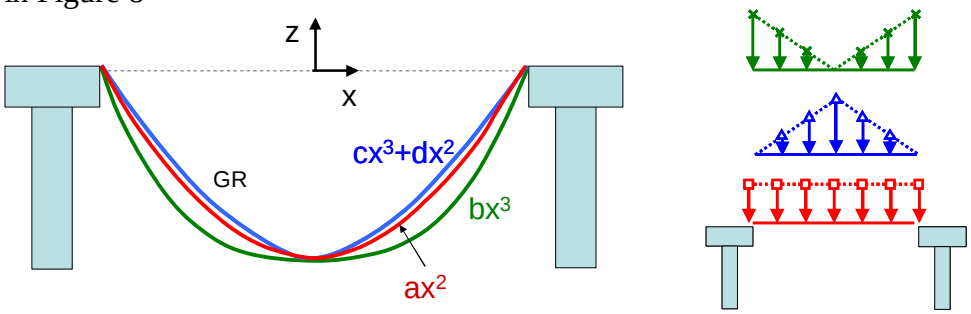

Figure 8. Relation between shape deformed GR (left) and load distribution (right)

The shape of the deformed GR is measured both by the liquid levelling system, and by scanning the surface of the sand layer below the GR, before and after the test. The results of both measurements, of several tests, are presented in Figure 9. From this, it should be concluded that the load distribution on the GR strip agrees best (at least) with the (green) inverse triangle of Figure 8. This is also confirmed by the direct measurements of the vertical load with extra force transducers on the GR strips, as shown in Figure 10 and by numerical calculations as shown by Den Boogert et al., 2012.

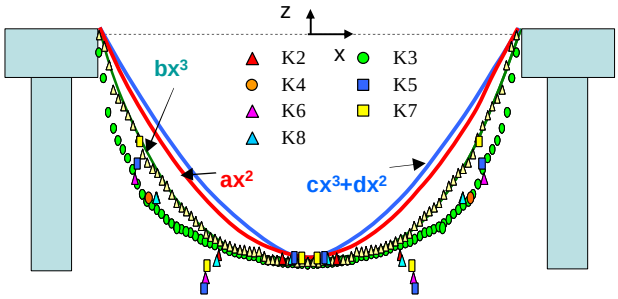

Figure 9. the measured shape of the GR agrees best with the third-order-polynomial

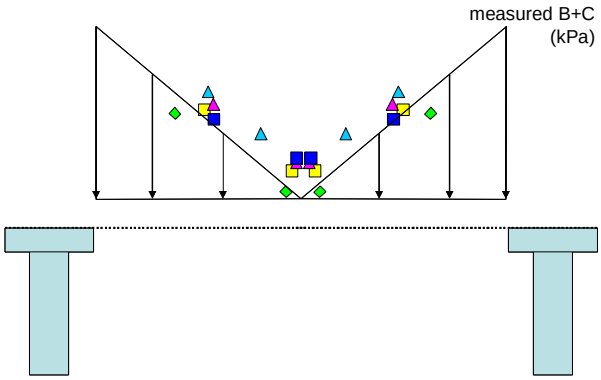

Figure 10. measured load distribution on the GR strip

Therefore, it is concluded that the distribution of the line load on the reinforcement strip between two piles tends to have the distribution of an inverse triangle. However, EBGEO calculations are based on a triangular-shaped line load.

Considering the subsoil support of the GR strip, EBGEO mobilises only part of the subsoil, namely the area below the GR strips between the piles. Van Eekelen et al., (2011c) gives the equations to increase the supporting subsoil area to the entire available area below the GR and for the implementation of the inverse triangle.

Figure 11 shows the results of modifying CUR/EBGEO-step 2 by improving both the subsoil support and the load distribution. The figure shows that this gives a much better agreement with the measurements, and 19-26% less GR strain (and therefore required GR strength) than the EBGEO assumptions.

6 CONCLUSIONS

Purpose of the tests series was to find an explanation why the calculated GR strains exceed the GR strains measured in the field.

Five starting points were adopted, which resulted in the following test set-up features:

1. Load parts A, B and C (Figure 4) were measured separately and the GR strain were measured to make it possible to evaluate the two calculation steps separately. For the measurement of the GR strain, a new measurement system was developed, using a bicycle gear cable. The results of this system improved during the test series.
2. A soaked, watertight wrapped foam cushion was applied to simulate the behaviour of the soft subsoil. This made it possible to control the subsoil support and evaluate the influence of consolidation of the subsoil.
3. Include GR to study the behaviour of a GR reinforced piled embankment.
4. Apply a granular of broken construction material, to model the frictional fill realistically.
5. Apply a rather high surcharge load, to get a realistic stress level in the arching area.

For the test conditions (static load, laboratory scale), it was found that consolidation of the subsoil results in an increase of arching. This is not in agreement with the current calculation models. Loading on the GR is concentrated on the strips lying above and between adjacent piles (the “GR strips”) which is in agreement with the current calculation models. The measured load on a GR strip has the distribution of an inverse triangle, although the load may be even more concentrated around the pile caps than this indicates. This is not in agreement with the current calculation models. Implementing this in the CUR/EBGEO calculation model results in 19-26% less GR strain.

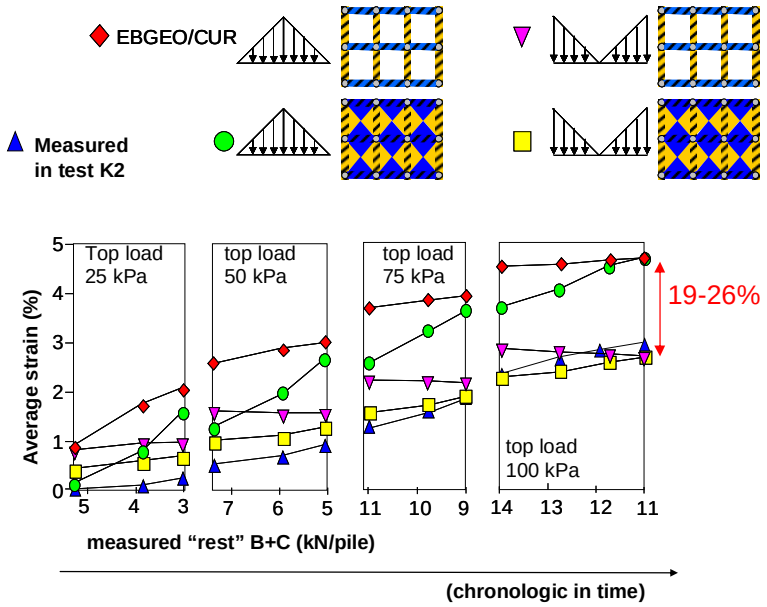

Figure 11. Comparison measurements and calculations step 2, effect of modifications CUR/EBGEO calculation model: a. modification load distribution (from triangular shape to inverse triangular shape) and b. modification subsoil support (from below GR strip only to below entire, diamond shaped GR area)

REFERENCES

Blanc, M. Rault, G., Thorel, L. and Almeida, M. (2012), Investigation in centrifuge of load transfer mechanisms above a rigid inclusions network, to be published in the *Proceedings of EuroFuge 2012*, Delft, the Netherlands

BS8006-1: 2010. *Code of practice for strengthened/reinforced soils and other fills.* British Standards Institution, ISBN 978-0-580-53842-1

CUR 226, 2010, *Ontwerprichtlijn paalmatrassystemen (Design guideline piled embankments)*. ISBN 978-90-376-0518-1 (in Dutch)

Chen, Y.M., Cao, W.P., Chen, R.P., 2008. An experimental investigation of soil arching within basal reinforced and unreinforced piled embankments. *Geotextiles and Geomembranes, 26 (2008)* 164-174.

Den Boogert, T.J.M., Van Duijnen, P.G., Peter, M.G.J.M. and Van Eekelen, S.J.M., 2012, Paalmatrasproeven II, Eindige elementenberekeningen, *GeoKunst, GeoTechniek January 2012*, pp. 52-57, in Dutch

EBGEO, 2010. *Empfehlungen für den Entwurf und die Berechnung von Erdkörpern mit Bewehrungen aus Geokunststoffen – EBGEO, 2*. Auflage, German Geotechnical Society, ISBN 978-3-433-02950-3 (in German). Also available in English: *Recommendations for Design and Analysis of Earth Structures using Geosynthetic Reinforcements – EBGEO, 2011*. ISBN 978-3-433-02983-1 and digital in English ISBN 978-3-433-60093-1).

Ellis, E., Aslam, R., 2009a. Arching in piled embankments. Comparison of centrifuge tests and predictive methods, part 1 of 2. *Ground Engineering, June 2009*, pp 34-38.

Ellis, E., Aslam, R., 2009b. Arching in piled embankments. Comparison of centrifuge tests and predictive methods, part 2 of 2. *Ground Engineering, July 2009*, pp 28-31.

Farag, G.S.F., 2008. *Lateral spreading in basal reinforced embankments supported by pile-like elements.* Schiftenreihe Getechnik, Heft 20, Universität Kassel, März 2008.

Halvordson , K.A., Plaut, R.H., Filz, G.M., 2010. Analysis of geosynthetic reinforcement in pile-supported embankments. Part II: 3D cable-net model. *Geosynthetics International, Volume 17, Issue 2,* pages 68 –76, ISSN: 1072-6349, E-ISSN: 1751-7613.

Haring, W., Profittlich, M. & Hangen, H., 2008. Reconstruction of the national road N210 Bergambacht to Krimpen a.d. IJssel, NL: design approach, construction experiences and measurement results. In: *Proceedings 4th European Geosynthetics Conference*, September 2008, Edinburgh, UK.

Heitz, C., 2006. *Bodengewölbe unter ruhender und nichtruhender Belastung bei Berücksichtigung von Bewehrungseinlagen aus Geogittern*. Schriftenreihe Geotechnik, Uni Kassel, Heft 19 November 2006 (German)

Lawson, C.R., 2012, Role of Modelling in the Development of Design Methods for Basal Reinforced Piled Embankments, to be published in the *Proceedings of EuroFuge 2012*, Delft, the Netherlands

Le Hello, B., 2007. *Renforcement par geosynthetiques des remblais sur inclusions rigides, étude expérimentale en vraie grandeur et analyse numérique*. PhD thèses, l'université Grenoble I, (in French).

Hewlet, W.J., Randolph, M.F. Aust, M.I.E, 1988. Analysis of piled embankments. *Ground Engineering*, April 1988, Volume 22, Number 3, 12-18.

Horgan, G.J., and Sarsby, R.W., 2002. The arching effect of soils over voids and piles incorporating geosynthetic reinforcement. *Geosynthetics, 7th ICG*, Delmas, Gourc & Girard (eds) Swets & Zeitlinger, Lisse ISBN 90 5809 523 1, pp 373-378.

Jenck, O., Dias, D., and Kastner, R., 2009. Discrete element modelling of a granular platform supported by piles in soft soil – Validation on a small-scale model test and comparison to a numerical analysis in a continuum. *Computers and Geotechnics 36* (2009) 917–927.

Jones, B.M., Plaut, R.H., Filz, G.M., 2010. Analysis of geosynthetic reinforcement in pile-supported embankments. Part I: 3D plate model. *Geosynthetics International, Volume 17, Issue 2*, pages 59 –67, ISSN: 1072-6349, E-ISSN: 1751-7613.Low, B.K., Tang, S.K., and Chao, V., 1994. Arching in piled embankments. *J. of Geo. Eng., ASCE, 120(11)*, pp. 1917-1938.

Van Eekelen, S.J.M., Bezuijen, A., Oung, O., 2003. Arching in piled embankments; experiments and design calculations, in: *Proceedings of ICOF conference*, September 2003, Dundee, Scotland.

Van Eekelen, S.J.M., Jansen, H.L., Van Duijnen, P.G., De Kant, M., Van Dalen, J.H., Brugman, M.H.A., Van der Stoel, A.E.C., Peters, M.G.J.M., 2010a. The Dutch Design Guideline for Piled Embankments. In: *Proceedings of 9 ICG, Brazil*, pp. 1911-1916.

Van Eekelen, S.J.M.; Bezuijen, A. and Van Tol, A.F., 2011a. Analysis and modification of the British Standard BS8006 for the design of piled embankments. *Geotextiles and Geomembranes* 29 (2011) pp.345-359.

Van Eekelen, S.J.M., Bezuijen, A., Lodder, H.J., van Tol, A.F., 2011b. Model experiments on piled embankments. Part I, *Geotextiles and Geomembranes*. doi:10.1016/j.geotexmem.2011.11.002

Van Eekelen, S.J.M., Bezuijen, A., Lodder, H.J., Van Tol, A.F., 2011c. Model experiments on piled embankments, part II. *Geotextiles and Geomembranes*, doi:10.1016/j.geotexmem.2011.11.003.

Zaeske, D., 2001. *Zur Wirkungsweise von unbewehrten und bewehrten mineralischen Tragschichten über pfahlartigen Gründungselementen*. Schriftenreihe Geotechnik, Uni Kassel, Heft 10, February 2001 (in German).